Bulg. J. Phys. **45** (2018) 67–75

Study of 6 MV Photon Beam Dose Profiles, Investigation and Evaluation of Scattered photons and Electrons Contamination Effects on Beam Dose Profiles

M. Bencheikh[1], **A. Maghnouj**[1], **J. Tajmouati**[1], **A. Didi**[1], **A. Lamrabet**[1], **Y. Benkhouya**[2,3]

LISTA Laboratory, Physics Department, Faculty of Sciences Dhar El-Mahraz, University of Sidi Mohamed Ben Abdellah, Fez, Morocco

[2]Radiotherapy Department, Al Kawtar Clinic, Fez, Morocco

[2]Nuclear physics laboratory, Faculty of Sciences Agdal, University of Mohammed V, Rabat, Morocco

Received *18 September 2017*

Abstract. In this study we have investigated the scattered photons and electrons contamination effects on dose profiles due beam modifiers and jaw system motion.

Firstly, we have calculated the increasing relative dose on beam profile as a function of field size and depth along central beam axis and we have normalized the increasing relative dose on beam profile to the increasing relative dose of standard filed size of 10×10 cm^2.

Secondly, we have calculated the width of dose profiles as function of field size and depth; then we have investigated the beam symmetry on central beam axis and the jaw motion effects on delivered dose, we have calculated two parameters: the normalized width and the width difference between left and right width of dose profiles as a function of field size and depth.

We concluded that scattered photons and electrons contamination effects on dose profiles must be taken in consideration when the physicians treat the tumor because the dose profile peaks have an increasing in dose that increased with irradiation field size and in shallow depths (10 cm) in water phantom 10×10 cm^2 due to scattered photons and electrons contamination coming from beam modifiers near the phantom surface.

This study was an experimentation investigation of delivered dose from linear accelerator; our results will be an investigation by Monte Carlo method to improve the dosimetry and linac in the future.

PACS codes: 87.50.cm, 87.10.Rt, 87.50.st

1 Introduction

Radiotherapy treatment basic purpose is the irradiation of target volume of cancerous cells while minimizing the amount of radiation absorbed in healthy cells. The beam shaping is an important element to reduce the absorbed dose in healthy tissue and critical structures. The penetration of radiation beam is a factor of interest; the quality of penetration of radiation beam depends on voltage peak and applied filtration. Medical linear accelerators delivering photon beams are equipped with flattening filter to ensure the production of homogeneous distributions of doses for clinical use. The dose investigations were done in our previous works [10-12], these investigations were done for percentage depth dose (PDD) and beam dose profiles.

Medical linear accelerators are generally designed to provide homogeneous photon beam to variety of irradiation field sizes and shapes using collimation system. The collimation system includes primary collimator and secondary collimator. Secondary collimators or conventional collimators are also called the jaws are used to shape a rectangular field for tumor treatment. The dose profile is a function of off axis distance and irradiation field size. The dose profiles at different depths are needed for good study of dosimetry with off-axis distance x from central beam axis to beam edge. For good interpretation of experimentation measurements, dose profiles are obtained by using a water phantom with high technical and clinical conditions of experiments.

The objective of this study was to investigate and evaluate the scattered photons and contamination electron effects on dose profiles for flattening filter and collimation system by examining the dose profiles as function of depth along central beam axis and off-axis distance. The backscattering effects are very high for the large filed sizes and the later are more stable depending on the depth, however, the backscattering effects are very low for the small filed sizes, they are unstable as function of the depth along central beam axis. This study was an experimentation investigation of delivered dose from linear accelerator; our results will be an investigation by Monte Carlo method to improve the dosimetry and linac in the future.

We have tied many results between them in this work for make in evidence many things and effects of photon beam modifies for Varian Clinac 2100 using an experimental study of dosimetry data determined inside the radiotherapy department Al kawtar clinic in Fez Morocco.

2 Materials and Methods

After tuning the required parameters for this study as source-to-surface distance (SSD) at 100 cm and photon beam energy of 6 MV, dose profiles were measured by PTW scanner. The width of scans is perpendicular to central beam axis and

depends on both irradiation field size and depth along central beam axis in the tank (due to beam divergence) and it must be sufficiently large to include the beam edges.

Dose profile measurements were performed for 6 MV photon beam produced by Varian Clinac 2100 in a water phantom at depth of 1.5 cm, 5 cm, 10 cm, 20 cm and 30 cm for field sizes A_d of 6×6 cm^2, 10×10 cm^2, 20×20 cm^2, 30×30 cm^2. All measurements were performed with same clinical and technical conditions of experimentation and measurement. Then we have normalized the dose profiles to 100% on central beam axis for all studied irradiation field sizes and at different depths on beam central axis.

First step, we have proceeded to evaluate the increasing in dose on beam dose profiles; for good way to do it, the off-axis distance was normalized $N_{\text{Off-axis}}$ using the flowing formula (1):

$$N_{\text{Off-axis}} = \frac{2x}{a_d}\,, \tag{1}$$

where a_d stands for side of square field size at a depth d, x – off-axis distance.

Second step, the increasing in dose (ID) was evaluated with depth d for a field size A_d according to the formula

$$ID(d, A_d) = \max\left(D(x, d) - D(0, d)\right)\,, \tag{2}$$

where $D(0, d)$ is the dose on beam central axis for field size A_d at a depth d, $D(x, d)$ – dose at point x perpendicularly away from central beam axis for field size A_d at a depth d.

We have worked on normalized dose profiles to dose on central beam axis. So we have calculated the increasing relative dose (IRD) according to the following formula:

$$IRD\left(d, A_d\right) = \max RD(dA_d) - 100 \tag{3}$$

where $IRD(d, A_d)$ stends for the increasing in relative dose for field size A_d at a depth d; $RD(d, A_d)$ – relative dose for filed size A_d at a depth d.

Thereafter, we have normalized the increasing in relative dose for each field size to the increasing in relative dose of 10×10 cm^2 field size according to the following formula:

$$NIRD(d, A_d) = \frac{IRD(d, A_d)}{IRD(d, 10 \times 10\ \text{cm}^2)}\,, \tag{4}$$

where $NIRD(d, A_d)$ is the normalized increasing in relative dose of field size of A_d at a depth d.

Third step; we have demonstrated that the jaw motion have effects on dose profiles as a function of field size and depth. Thereafter, we proceeded to calculate

the left widths W_l of dose profile and the right widths W_r of dose profile for dose of 80% of dose maximum, then, we have calculated the normalized width W_n according to formula (5):

$$W_n = \left| \frac{W_l - W_r}{W_l + W_r} \right|. \tag{5}$$

In normal use of the secondary collimator, each pair of jaws is coupled to provide symmetric rectangular fields centered about central beam axis. In our study, we worked on square fields, open (not wedged), symmetrical, and centered about central beam axis.

3 Results and Discussion

To shows the flattening filter effects on beam dose profiles, Figure 1 shows dose profiles for field sizes of 6×6 cm^2, 10×10 cm^2, 20×20 cm^2 and 30×30 cm^2 cm^2 at a depth of 1.5 cm as a function of normalized off-axis distance.

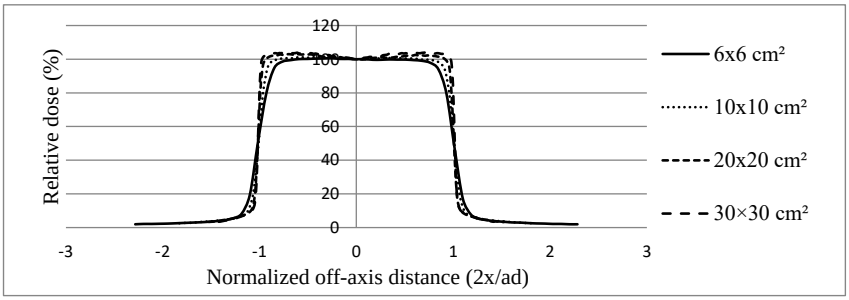

Figure 1. Dose profiles as functions of normalized off-axis distance for field size of 6×6 cm^2, 10×10 cm^2, 20×20 cm^2 and 30×30 cm^2 cm^2 at a depth of 1.5 cm.

The peaks or increasing in relative appeared at the beam edge, where $2x/ad = 1$ on dose profiles (Figure 1). It can be seen that the increasing in relative dose increased with field sizes. The incrassating in relative dose were produced by flattening filter design and geometry [3,6,8,9]. Table 1 shows the increasing in relative dose and the normalized increasing in relative dose with field size.

Normalized increasing in relative dose increased with field size, for making good interpretation of results in Table 1, Figure 2 shows variation of normalized increasing in relative dose.

It can be seen from Figure 2 that the normalized increasing in relative dose curves presented the peaks at depth of 10 cm for all filed size over than field size of 10×10 cm^2 [3,6,8,9]. The peak values increased with field size, the increasing in relative dose for the large field size due to the scattered photons

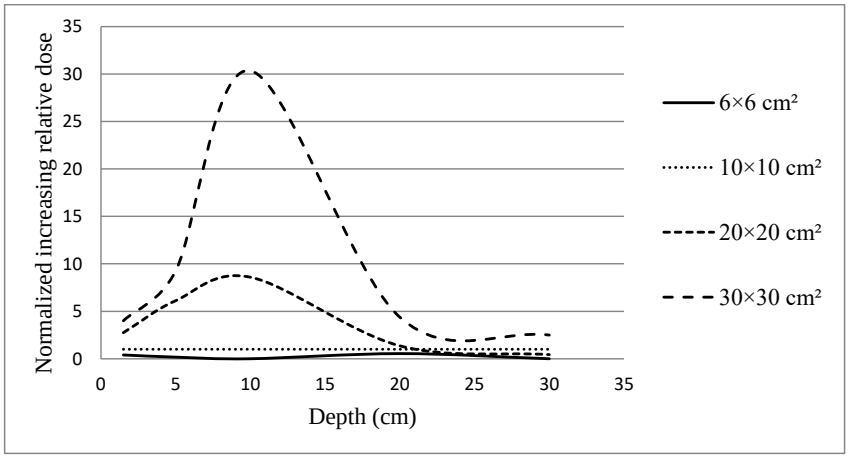

Figure 2. Variation of normalized increasing in relative dose as a function of depth for field size of 6×6 cm^2, 10×10 cm^2, 20×20 cm^2 and 30×30 cm^2 cm^2 at a depth of 1.5 cm.

that it increased with field size by increasing the material jaw surface of photon interactions. In our study we have quantified these effects; so, for filed size of 20×20 cm^2, the increasing relative dose was 8.59% of the increasing in relative dose of 10×10 cm^2. Therefore, backscattering effects for field size of 20×20 cm^2 were more by 8.59 of backscattering effects of field size of 10×10 cm^2 cm^2 (Figure 2).

Electrons contamination effects were also investigated due to jaw motions to define the irradiation field size, and then we have shown that the variation of normalized width W_n as a function of depth and field size (Table 2)

For jaw motion investigation, the normalized widths were evaluated with square side of field size (Figure 3).

The normalized width was high for small field sizes; the curves of this quantity

Table 1. Increasing in relative dose variation for field size of 6×6 cm^2, 10×10 cm^2, 20×20 cm^2 and 30×30 cm^2 cm^2 at a depth of 1.5 cm.

Field size A_d (cm^2)	Increase in relative dose on left beam profile	Increase in relative dose on right beam profile	Averaged i increase in relative dose	Normalized increase in relative dose
6×6	0.7	0.1	0.4	0.4
10×10	1.2	0.8	1	1
20×20	2.9	2.6	2.75	2.75
30×30	4	4	4	4

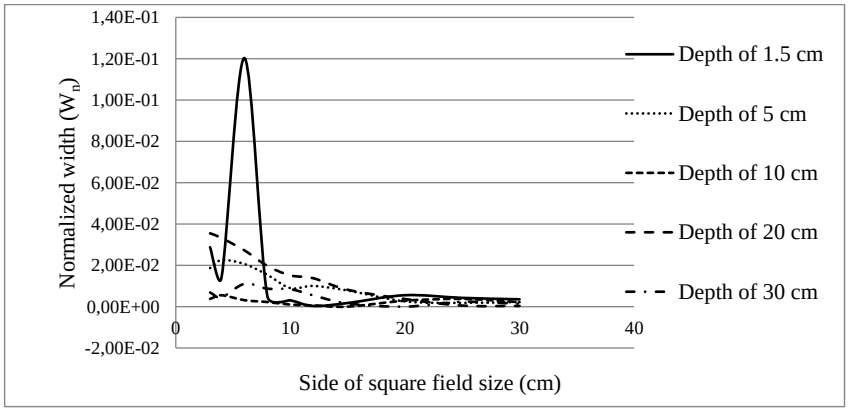

Figure 3. Variation of normalized width W_n as a function of square side of field size; depth of 1.5 cm, 5 cm, 10 cm, 20 cm and 30 cm in water phantom.

are spaced between them as a function of depth. However, the normalized width is very small for field size more than 20×20 cm^2 because the curves are close for all studied depths (Figure 3).

In small field sizes, the jaws are close for each pair jaw, the primary photons interacted with jaw inner surface material and electrons contamination passed through the phantom surface; thereafter, electrons contamination density was high and its dosimetry contribution in total dose delivered was important, so they affected dose profile curves for small field sizes (Figure 3). In large field sizes, the jaws are away from each other in a pair jaw, the phantom surface is large, so the density electrons contamination was low; hence, their dosimetric contribution to dose delivered was also low. So, the normalized width curves are close each to other along central beam axis.

For irradiation field symmetry investigation, the difference between left profile width and right profile width was evaluated. This quantity allowed us to investigate dose profile symmetry about the central beam axis with depth in water phantom. Figure 4 gives variation of difference between left profile width and

Table 2. Left profile width W_l, right profile width W_r and normalized width W_n for field size of 6×6 cm^2, 10×10 cm^2, 20×20 cm^2 and 30×30 cm^2 cm^2 at a depth of 1.5 cm.

Side of square field (cm)	Left width W_l (mm)	Right width W_r (mm)	Normalized width W_n
6	35.47	27.85	1.20×10^{-01}
10	48.15	47.86	3.08×10^{-03}
20	99.19	98.10	5.53×10^{-03}
30	150.08	149.02	3.54×10^{-03}

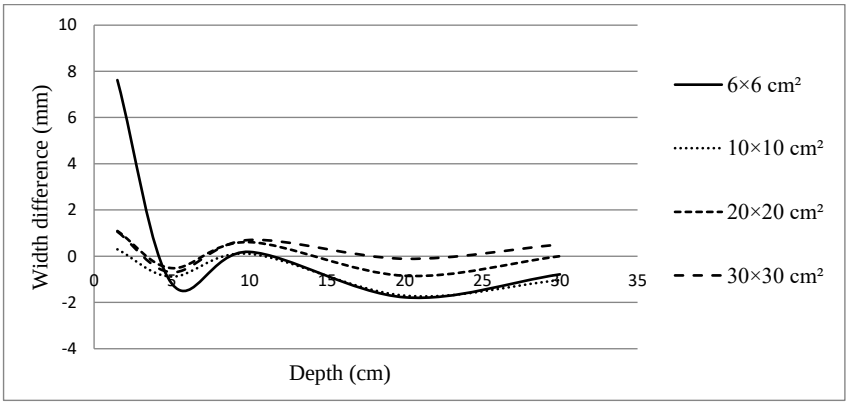

Figure 4. Variation of difference between left profile width W_l and right profile width W_r as a function of depth for field size of 3×3 cm^2, 4×4 cm^2, 6×6 cm^2, 8×8 cm^2, 10×10 cm^2, 12×12 cm^2, 15×15 cm^2, 20×20 cm^2, 25×25 cm^2, 30×30 cm^2 and 35×35 cm^2.

right profile width as a function of depth in water phantom for each field size.

The difference between left profile width and right profile width moved along central beam axis as a wave motion about the central beam axis for all studied field sizes. It can be seen in shallow depths, the curves are close between them but while depth increased in water phantom, space between curves increased also, that means the spot size of photon beam become more width with increasing depth; however, the amplitude variation of difference of width remained in interval from -2 mm to 2 mm along central beam axis (Figure 4).

Dose profiles are not symmetrical about the central axis that the theory gave. At some depths where differences of width were zero, dose profiles were symmetrical for each studied field size and they are not symmetrical elsewhere. The symmetry of dose profiles depends on irradiation field size and depth in phantom.

4 Conclusion

Our study aimed to make an experimental investigation of dosimetric contribution of scattered photons and electrons contamination on beam dose profiles and subsequently dose delivered. Normalized increasing in relative have peak at a depth of 10 cm that it is flattening filter characterization in flattening and softening of photon beam that was reached a depth of 10 cm as mentioned in previous studies [3].

The increasing in relative dose for field size more than 20×20 cm^2 is very important than field size of 10×10 cm^2. For instance, we have found that the

increasing in relative dose at depth of 10 cm for t field size of 25×25 cm^2 was almost 20 times of the increasing in relative dose of field size of 10×10 cm^2, but the normalized increasing in relative dose is very low for all filed sizes at a depth of 20 cm along central beam axis (Figure 3 and 4). These values must be taken in consideration when the physicians treat the tumor. The dose profile peaks have an increasing in dose that increased with irradiation field size and in shallow depths (10 cm) in water phantom 10×10 cm^2 due to scattered photons and electrons contamination coming from beam modifiers near the phantom surface [1-5,7,9], our results are consistent with study of Young-Jae Kim et al. [6].

In this study, we have shown that the jaw motion effects were very depending on irradiation field size. Dosimetric contribution of electrons contamination to delivered dose is more important in small field sizes and it is almost zero in field sizes more than 20×20 cm^2.

We have also shown that dose profiles are not symmetrical about central beam axis as fields are symmetrical and centered about central beam axis except at certain depths in the water phantom where the difference was zero. And the difference of width spread in interval from -2 mm to 2 mm.

We concluded that scattered photons and electrons contamination effects on dose profiles must be taken in consideration when the physicians treat the tumor because the dose profile peaks have an increasing in dose that increased with irradiation field size and in shallow depths (10 cm) in water phantom 10×10 cm^2 due to scattered photons and electrons contamination coming from beam modifiers near the phantom surface [1-5,7,9], our results are consistent with study of Young-Jae Kim et al. [6].

Acknowledgement

The authors would like to thank Varian medical systems to allow us to use the dose profiles commissioning data of Varian Clinac 2100, and give us this opportunity to study the Varian linear accelerator technology and to participate in its future development, our study is one among many study over the world in this field.

References

[1] P. Mayles, A. Nahum, and J.C. Rosenwald (2007) "*Handbook of Radiotherapy Physics Theory and Practice*" (Taylor & Francis group, LCC, USA) pp 452-480.

[2] D.S. Chang, F.D. Lasley, I.J. Das, M.S. Mendonca, and J.R. Dynlacht (2014) "*Basic Radiotherapy Physics and Biology*" (Springer, New York) pp 77-92.

[3] E.B. Podgorsak (2005) "*Radiation Oncology Physics: A Handbook For Teachers And Students*" (IAEA, Vienna) pp 161-216.

[4] C.J. Karzmark, C.S. Nunan, and E. Tanabe (1993) "*Medical Electron Accelerators*" (Library of Congress, USA) pp 147-148.

[5] E.B. Podgorsak (2014) "*Compendium to Radiation Physics for Medical Physicists*" (Springer-Verlag Berlin Heidelberg) pp 1075-1099.

[6] Y.J. Kim, K.R. Dong, W.K. Chung, C.S. Lim, C.S. Jeong, and Y.J. Seo (2015) *J. Korean Phys. Soc.* **64** 917-922; doi: 10.3938/jkps.64.917.

[7] G. Liu, T. Van Doorn, and E. Bezak (2002) *Australas. Phys. Eng. Sci. Med.* **25** 58-66; doi: 10.1007/BF03178467.

[8] F.C. Henriquez and S.T. Vargas-Castrillón (2007) *Australas. Phys. Eng. Sci. Med.* **30** 147-151; doi: 10.1007/BF03178420.

[9] Y. Sitti, I.G.E. Dirgayuss, F.R. Mohamad, C.X.S. Roger, H. Freddy, and A. Idam (2016) *J. Smart Sci.* **4** 15-28; doi: 10.1080/23080477.2016.1195609.

[10] M. Bencheikh, A. Maghnouj, J. Tajmouati, and Y. Benkhouya (2016) *Mor. J. Chem*. **4** 996-1003/

[11] M. Bencheikh, A. Lamrabet, A. Didi, A. Maghnouj, and J. Tajmouati (2016) *Mor. J. Chem*. **4** 722-730.

[12] M. Bencheikh, A. Maghnouj, and J. Tajmouati (2017) *Appl. J. Envir. Eng. Sci.* **3** 23-29.